Translational Oncology
www.transonc.com

Volume 6 Number 4 August 2013 pp. 420–428 420

Individual Profiling of Circulating Tumor Cell Composition and Therapeutic Outcome in Patients with Hepatocellular Carcinoma[1]

Ivonne Nel*, Hideo A. Baba†, Judith Ertle‡, Frank Weber§, Barbara Sitek¶, Martin Eisenacher¶, Helmut E. Meyer¶, Joerg F. Schlaak‡ and Andreas-Claudius Hoffmann*

*Department of Medical Oncology, Molecular Oncology Risk-Profile Evaluation, West German Cancer Center, University Hospital of Essen, Essen, Germany; †Department of Pathology and Neuropathology, University Hospital of Essen, Essen, Germany; ‡Department of Gastroenterology and Hepatology, University Hospital of Essen, Essen, Germany; §Department of General, Visceral and Transplantation Surgery, University Hospital of Essen, Essen, Germany; ¶Medical Proteome-Center, Ruhr-University Bochum, Bochum, Germany

Abstract

BACKGROUND AND AIMS: Circulating tumor cells (CTCs) have been proposed as a monitoring tool in patients with solid tumors. So far, automated approaches are challenged by the cellular heterogeneity of CTC, especially the epithelial-mesenchymal transition. Recently, Yu and colleagues showed that shifts in these cell populations correlated with response and progression, respectively, to chemotherapy in patients with breast cancer. In this study, we assessed which non-hematopoietic cell types were identifiable in the peripheral blood of hepatocellular carcinoma (HCC) patients and whether their distribution during treatment courses is associated with clinical characteristics. *METHODS:* Subsequent to few enrichment steps, cell suspensions were spun onto glass slides and further characterized using multi-immunofluorescence staining. All non-hematopoietic cells were counted and individual cell profiles were analyzed per patient and treatment. *RESULTS:* We detected a remarkable variation of cells with epithelial, mesenchymal, liver-specific, and mixed characteristics and different size ranges. The distribution of these subgroups varied significantly between different patient groups and was associated with therapeutic outcome. Kaplan-Meier log-rank test showed that a change in the ratio of epithelial to mesenchymal cells was associated with longer median time to progression (1 *vs* 15 months; $P = .03$; hazard ratio = 0.18; 95% confidence interval = 0.01–2.75). *CONCLUSIONS:* Our data suggest that different CTC populations are identifiable in peripheral blood of HCC patients and, for the first time in HCC, that these individual cell type profiles may have distinct clinical implications. The further characterization and analysis of patients in this ongoing study seems to be warranted.

Translational Oncology (2013) 6, 420–428

Address all correspondence to: Andreas-Claudius Hoffmann, MD, Assistant Professor of Experimental Oncology, Department of Medical Oncology, Molecular Oncology Risk-Profile Evaluation, West German Cancer Center, University Hospital Essen, Hufelandstrasse 55, 45147 Essen, Germany. E-mail: hoffmann@more-oncology.com

[1]This project is financed by funds of the "Ziel 2—Programm NRW 2007-2013, Bio.NRW," the European fund for regional development (EFRE, "Europäischer Fonds für regionale Entwicklung," "Investition in unsere Zukunft"), and funds from the Ministry of Innovation, Science and Research of North Rhine-Westphalia, Germany; this project was also presented at the "Advances in Circulating Tumour Cells (ACTC)" Conference in Athens in 2012. No author has any conflict of interest that is relevant to the manuscript.
Received 10 March 2013; Revised 30 April 2013; Accepted 2 May 2013

DOI 10.1593/tlo.13271

Introduction

Hepatocellular carcinoma (HCC) is associated with a poor prognosis and is among the five most common malignancies worldwide with an increasing incidence [1,2]. Curative therapeutic options are limited to early stages and include mostly resection or orthotopic liver transplantation if patients present with cirrhosis [3,4]. High recurrence rates after resection and liver transplantation, most likely because of minimal residual disease [5,6], and the fact that the majority of patients are diagnosed in an advanced stage make palliative, often localized approaches including selective internal radiation therapy and transcatheter arterial chemoembolization necessary [7,8]. Up to now, there are no reliable early markers of relapse or response to surgical or interventional therapy. Serum-based markers like alpha-fetoprotein (AFP), des-gamma-carboxyprothrombin, or the lectin 3 fraction of AFP (AFP-L3) are incapable of predicting the clinical outcome with high accuracy and reproducibility [9]. Tissue-derived molecular markers lack the possibility of monitoring the patient during or after treatment, because this would require repeated biopsies and hence increased risks for the patient. Therefore, the development of minimally invasive diagnostic methods is necessary.

Circulating tumor cell (CTC), detected in the peripheral blood of HCC patients, may represent a possible solution for this diagnostic dilemma. Though these cells have been frequently described in breast and lung cancers [10–12], only few studies reported on CTC in HCC patients using indirect methods like quantitative real-time reverse transcription–polymerase chain reaction or direct visualization of circulating epithelial cells [13–17]. The main obstacle to the broad clinical application of available automated CTC detection methods is the high plasticity and variability of these cells among others due to the epithelial-mesenchymal transition (EMT) as has been very recently shown by Yu and colleagues in breast cancer [18].

In this ongoing study, we wanted to scrutinize the hypothesis that a large variety of circulating non-hematopoietic cells exist in the peripheral blood of patients with HCC and that these cell types change during treatment and whether these changes may implicate resistance to therapy.

Materials and Methods

Study Population and Informed Consent

Patients with solid malignancies that received anticancer treatment in our hospital were consecutively included in this study after agreeing and signing a written informed consent in accordance with the requirements of our institution's board of ethics (Internal Reference No. 12-5047-BO). For this feasibility study, we tested the first 11 patients with a follow-up of at least 6 months. There were no inclusion criteria besides evaluable progression time and either being resected or receiving local ablative or systemic treatment. Patients with watch and wait were assessed but not included in outcome-related statistics at the time being. The clinicopathologic data of the patients used for CTC quantification is listed in Table 1.

Table 1. Patient Demographics for Quantification.

Demographic	Patients (n = 11)	
	No.	%
Tumor size (mm)		
Median	49	
Range	30–170	
Child status		
A	9	82
B	2	18
Cirrhosis	7	64
Chronic hepatic viral infection		
HBV	2	18
HCV	4	36
Age		
Median, years	70	
Range	42–85	
Therapy		
Watch and wait	3	27
Selective internal radiation therapy	5	45
Transcatheter arterial chemoembolization	1	9
Resection	1	9
Nexavar	1	9
Response		
Stable disease	4	36
Progressive disease	4	36
Time to progression (months)		
Median	3	
Range	0–19	

Blood Samples

Twenty milliliters of citrated peripheral blood from HCC patients was drawn during treatment visits in the outpatient unit of our liver tumor center, stored at room temperature, and processed within 24 hours after collection. We employed a negative selection strategy to enrich and detect CTC. Hematopoietic cells were depleted using anti-CD45 immunomagnetic beads leading to a bead-free cell suspension that was then used for CTC type detection by immunofluorescence staining against various epithelial [e.g., pan-cytokeratin (pan-CK)] and mesenchymal markers (e.g., vimentin, N-cadherin).

Cell Culture and Spiking Experiments

HCT 116 and HepG2 cell lines were obtained from American Culture Type Collection (ATCC, Rockville, MD) and maintained according to ATCC guidelines. For method validation, we used 20 ml of peripheral blood from healthy donors spiked with 100 HCT 116 cells. Spiked blood samples were processed using density gradient centrifugation and immunomagnetic enrichment strategy as described below. HepG2 cells were mixed with peripheral blood mononuclear cells (PBMNCs) from healthy donors and served as positive and negative controls for immunofluorescence staining. Gastrointestinal stromal tumor cells GIST 882 were a kind gift from Dr Bauer (Department of Medical Oncology, University Hospital Essen). Aliquots of GIST 882 cells were washed, resuspended in phosphate-buffered saline (PBS), and spotted onto glass slides for subsequent immunofluorescence staining against mesenchymal markers.

Sample Preparation

Isolation of PBMNCs using density gradient centrifugation. Twenty milliliters of citrated peripheral blood was diluted with 10 ml of PBS and poured into a Leucosep tube (Greiner Bio-One, Frickenhausen, Germany) prepared with 16-ml Ficoll-Paque (GE Healthcare, Buckinghamshire, Great Britain) below the porous barrier. After density gradient centrifugation at 1600g at 20°C for 20 minutes without brake, the PBMNCs containing interphase above the barrier were transferred into a new tube, washed with 50 ml of PBS containing 0.5% BSA, and centrifuged at 300g at 20°C for 10 minutes. Subsequently, the supernatant was removed completely.

Tumor cell enrichment using immunomagnetic beads. Washed PBMNCs were resuspended in 1 ml of PBS containing 0.1% BSA and incubated with 25 µl of anti-CD45–coated immunomagnetic Dynabeads (Invitrogen, Carlsbad, CA) for 30 minutes. Hematopoietic cells except erythrocytes, platelets, and their precursor cells were bound to beads and separated by a magnetic particle processor (King Fisher mL; Thermo Fisher, Waltham, MA). The remaining cell suspension included bead-free pre-enriched tumor cells and was spun onto two glass slides per sample using the Cell Spin II centrifuge (Tharmac, Waldsolms, Germany), air dried, and subsequently fixated with 96% ethanol. Slides were stored at 4°C until subjected to immunocytochemical staining. For assessment of the depletion rate, PBMNCs were stained with trypan blue and enumerated using an automated cell counter (Countess; Invitrogen) before and after immunomagnetic separation. The results indicated an average CD45 depletion of 73%. By increasing the concentration of immunomagnetic beads, the depletion rate could be increased up to 95%, though with an increasing damage in respect to cell morphology.

Identification of Spiked HCT 116 Cells after Density Gradient Centrifugation and Immunomagnetic Enrichment Using Immunocytochemical Labeling

Detection of HCT 116 cells was performed using the Epimet kit (Micromet, Munich, Germany). The identification of epithelial cells is based on the reactivity of the murine monoclonal antibody (mAb) A45-B/B3, directed against a common epitope of CK polypeptides. The kit uses Fab fragments of the pan-mAb conjugated with alkaline phosphatase molecules. The method includes permeabilization of the cells by a detergent (5 minutes), fixation by a formaldehyde-based solution (10 minutes), binding of the conjugate mAb A45-B/B3–alkaline phosphatase to cytoskeletal CK (45 minutes), and formation of an insoluble red reaction product at the binding site of the specific conjugate (15 minutes). Subsequently, the cells were counterstained with Mayer's hematoxylin for 1 minute and finally mounted with Kaiser's glycerin/gelatin (Merck, Darmstadt, Germany) in Tris-EDTA buffer (Sigma, Deisenhofen, Germany). A conjugate of Fab fragment served as a negative control. For each test, a positive control slide with the colon carcinoma cell line HCT 116 was treated under the same conditions. The microscopic evaluation was carried out using the ARIOL System (Applied Imaging, Newcastle upon Tyne, United Kingdom) in the Department of Gynecology and Obstetrics (Essen, Germany) according to the International Society of Hematotherapy and Graft Engineering (ISHAGE) evaluation criteria and the disseminated tumor cells (DTC) consensus [19,20]. This automated scanning microscope and image analysis system consists of a slide loader, camera, computer, and software for the detection and classification of cells of interest based on particular color, intensity, size, pattern, and shape.

Identification of CTC Subtypes Using Multifluorescence Labeling

Immunofluorescence staining of epithelial, mesenchymal, liver-derived, and hematopoietic cells was carried out in the CD45-depleted pre-enriched tumor cell suspension. Briefly, the staining method included fixation of the cells in 4.5% paraformaldehyde for 15 minutes, washing in PBS, permeabilization with 1× Perm/Wash Buffer (BD Biosciences, Franklin Lakes, NJ) for 10 minutes, washing in PBS, blocking of unspecific antibody reactions by incubation with blocking solution containing 5% BSA for 30 minutes, binding of primary antibodies (final concentration, 5 µg/ml) either ASGPR1 rabbit mAb (ab42488; Abcam, Cambridge, United Kingdom) or pan-CK guinea pig polyclonal antibody (ABIN126062, antibodies-online) and epithelial cell adhesion molecule (EpCAM, E144) rabbit mAb (ab32392; Abcam) or vimentin (EPR3776) rabbit mAb (2707-1; Epitomics, Burlingame, CA) or N-cadherin (EPR1792Y) rabbit mAb (2019-1; Epitomics) for CTCs and anti-CD45 (MEM-28) mouse mAb (ab8216; Abcam) for hematologic cells overnight at 4°C, washing in 0.1% Tween, binding of secondary antibodies (fluorescein isothiocyanate–conjugated AffiniPure goat anti-rabbit and Cy3-conjugated AffiniPure goat anti-mouse or Alexa Fluor 647–conjugated AffiniPure F(ab′)2 fragment goat anti-guinea pig; Jackson ImmunoResearch, Hamburg, Germany) for 30 minutes at 37°C, and washing in 0.1% Tween. Subsequently, cells were stained with 4′6-diamidino-2-phenylindole dihydrochloride (DAPI; Sigma-Aldrich, St Louis, MO) for 10 minutes, mounted with anti-fading medium (Invitrogen), and stored in the dark until evaluation. For each test, a positive control slide with a mixture of human PBMNCs and the HCC cell line HepG2 was treated under the same conditions. Gastrointestinal stromal cells (GIST 882) were used as positive control for mesenchymal markers. Microscopic evaluation was carried out using the digital Keyence BZ9000 (Biorevo, Osaka, Japan) all-in-one fluorescence microscope with integrated camera and BZ-Analyzer Software. We used

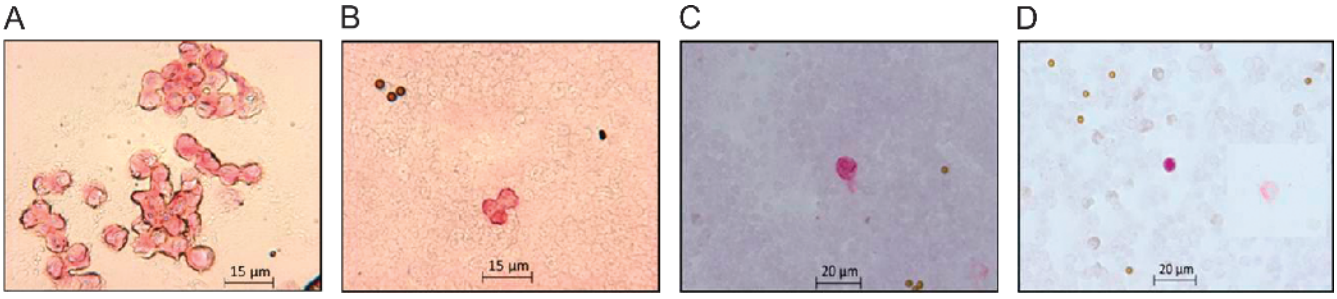

Figure 1. (A) Cultured HCT 116 cells were harvested, washed, and spun onto glass slides using the Cell Spin II centrifuge. Subsequently, they served as positive control for immunocytochemical staining against pan-CK (pink) using alkaline phosphatase. (B) Manual microscopic detection of spiked HCT 116 cells in peripheral blood from healthy donors enriched with density gradient centrifugation and negative enrichment through anti-CD45 immunomagnetic beads and stained against pan-CK. Pan-CK–positive cells are pink. Little brown round particles are immunomagnetic beads. (C) Detection of spiked HCT 116 cells using the ARIOL-SL automated scanning system resulted in a recovery rate of 100% after density gradient centrifugation and 43% after depletion of hematopoietic cells using anti-CD45–coated immunomagnetic beads. (D) Detection of pan-CK–positive cell in peripheral blood from HCC patient using the ARIOL-SL System.

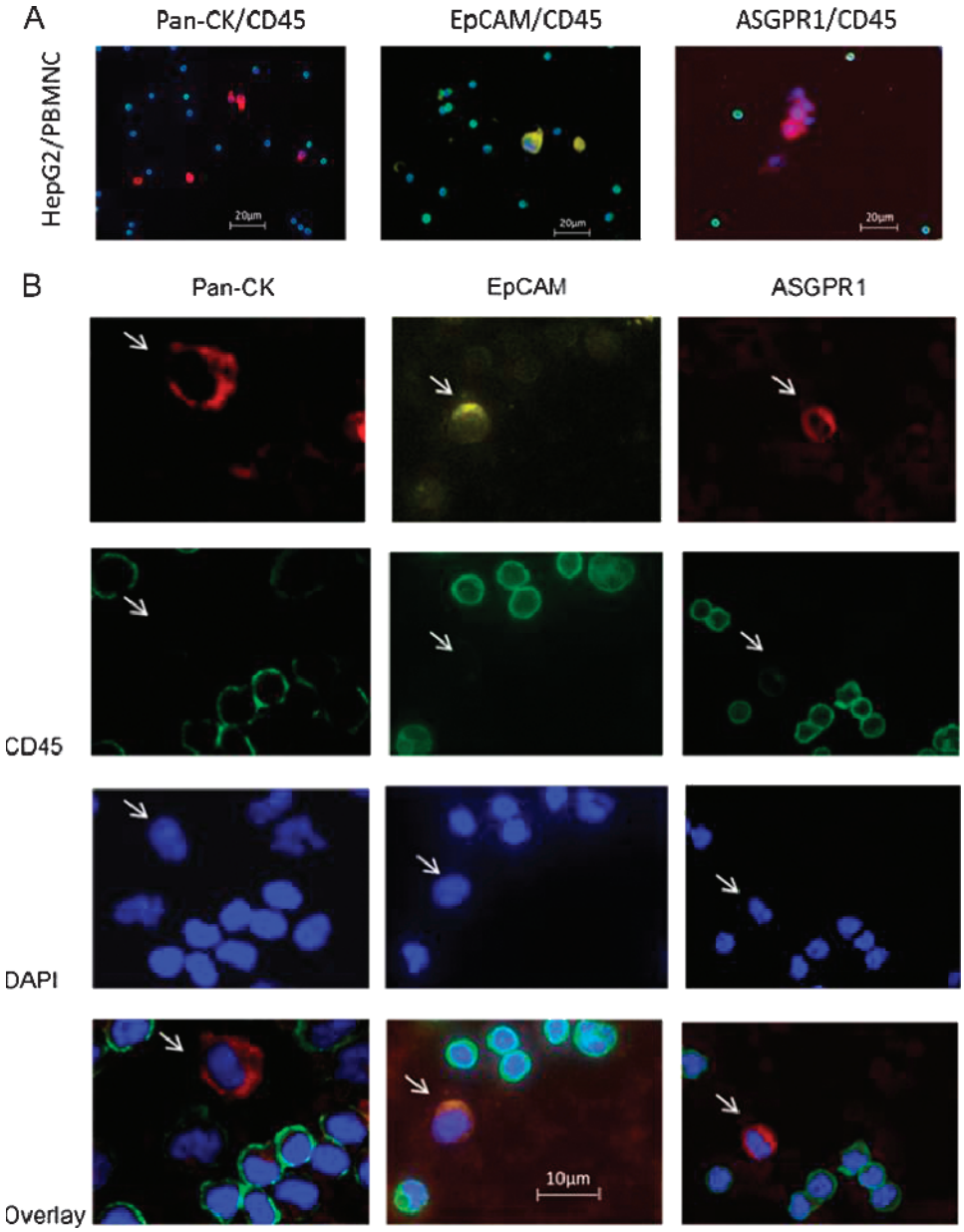

Figure 2. (A) Positive control consisting of PBMNCs mixed with HepG2 cells; stained against DAPI (blue) and epithelial or liver-specific markers: pan-CK (red) and CD45 (green); EpCAM (yellow) and CD45 (green); ASGPR1 (red) and CD45 (green). PBMNCs were positive for CD45 (green) and HepG2 cells were positive for pan-CK (red); EpCAM (yellow) and ASGPR1 (red). (B) CTC isolated from HCC patients stained against DAPI (blue) and pan-CK (red)/CD45 (green) and EpCAM (yellow)/CD45 (green) and ASGPR1 (red)/CD45 (green). Cells marked with a white arrow were considered as CTCs. They showed a DAPI-positive (blue)/CD45-negative staining and were positive for pan-CK (red) or EpCAM (yellow) or ASGPR1 (red).

pseudocolors to depict cells. Stained slides were manually examined and CTCs were detected within the same areas, each consisting of 10 visual fields using a ×20 magnification on both slides. Samples from five healthy donors were processed and examined under the same conditions to define a cutoff value for false-positive events.

Statistical Analysis

Statistical tests were performed according to previously published studies by our group [21–23]. Spearman rank correlation was used to examine associations between CTC subtypes and clinical characteristics of the patients. Associations of the cell type ratios and time to progression (TTP) were tested by the Kaplan-Meier method. Survival differences between patients with high and low cell type ratios were analyzed by the log-rank test. The level of significance was set to $P < .05$. All P values were based on two-sided tests. All statistical analyses were performed using the Software Packages SPSS for Windows (Version 19.0; SPSS Inc, Chicago, IL) and Medcalc, Version 12.3.0 (Mariakerke, Belgium).

Results

Enrichment Procedure

Analysis of the spiking experiments with 20 ml of whole blood and 100 epithelial HCT 116 cells using the automated scanning

microscope ARIOL-SL revealed a recovery rate of 100% after density gradient centrifugation. Subsequent depletion with immunomagnetic beads led to a significant lower recovery rate of 45% (Figure 1, *A*–*C*). Furthermore, we were able to detect CK-positive cells in the peripheral blood of HCC patients using this detection system (Figure 1*D*).

Immunofluorescence-based Identification of CTC Subtypes

For the investigation of cellular subtypes, a multistaining method was required to detect various epithelial, mesenchymal, and hematopoietic markers and to characterize different cell types. Therefore, we used multifluorescence staining for CTC subtype detection in HCC patients. A mixture of PBMNCs from a healthy donor spiked with epithelial cells from the HCC cell line HepG2 was used as positive control and negative control. Hematopoietic cells showed positive staining against CD45, whereas HepG2 cells were CD45-negative. HepG2 cells stained positive against the epithelial markers pan-CK and EpCAM and against the liver-specific ASGPR1 (Figure 2*A*). When examining samples from HCC patients, objects that showed a positive nuclear staining with DAPI, a negative staining for CD45, and a positive staining against pan-CK, EpCAM, or ASGPR1 were captured and considered as tumor cells (Figure 2*B*). We used GIST 882 cells as positive control for staining against the mesenchymal markers N-cadherin and vimentin (Figure 3*A*). In HCC blood samples, we detected cells with mesenchymal features such as N-cadherin+/CD45– and vimentin+/CD45– after negative isolation. We also detected cells showing both epithelial and mesenchymal characteristics such as N-cadherin+/CK+/CD45– and vimentin+/CK+/CD45– (Figure 3, *B* and *C*). In addition, we found cells that stained positive for potential markers of CTC and CD45 such as pan-CK+/EpCAM+/CD45+ as well as pan-CK+/EpCAM–/CD45+ cells (Figure 4*A* [24]). CTC profiles of each patient were examined and a ratio of mesenchymal to epithelial cells was conceived (Figure 4*B*). Although we detected a variety of cellular subtypes, we chose to summarize the total amount of N-cadherin–positive and vimentin-positive/CD45-negative cells in proportion to the total amount of CK-positive cells, respectively, after negative enrichment using CD45 depletion. We normalized the enumerated potential CTC against the total PBMNC number detected in the DAPI channel in each visual field and expressed the number of CTC per 1000 PBMNCs (Figure 4*C*). Analysis of samples from healthy donors revealed a cutoff for false-positive events at six CK-positive, one N-cadherin–positive, and two vimentin-positive/CD45-negative cells per 1000 PBMNCs after CD45 depletion.

Subtypes and Clinical Outcome

Spearman rank test resulted in a by trend significant association of TTP with the N-cadherin+/CK+ ratio ($P = .06$) and the vimentin+/CK+ ratio ($P = .07$), whereas there was no significant correlation of TTP of the total amount of CK-positive, N-cadherin–positive, and vimentin-positive cells. The total amount of N-cadherin–positive and vimentin-positive cells was associated to the amount of CK-positive cells ($P = .05$ and $P = .1$). Interestingly, 7 of 11 patients had cirrhosis, but there was no association to TTP ($P = .18$). Though, the total amount of CK-positive cells showed a by trend significant correlation to cirrhosis ($P = .1$; Figure 5*A*) and the ratio of N-cadherin+/CK+ cells

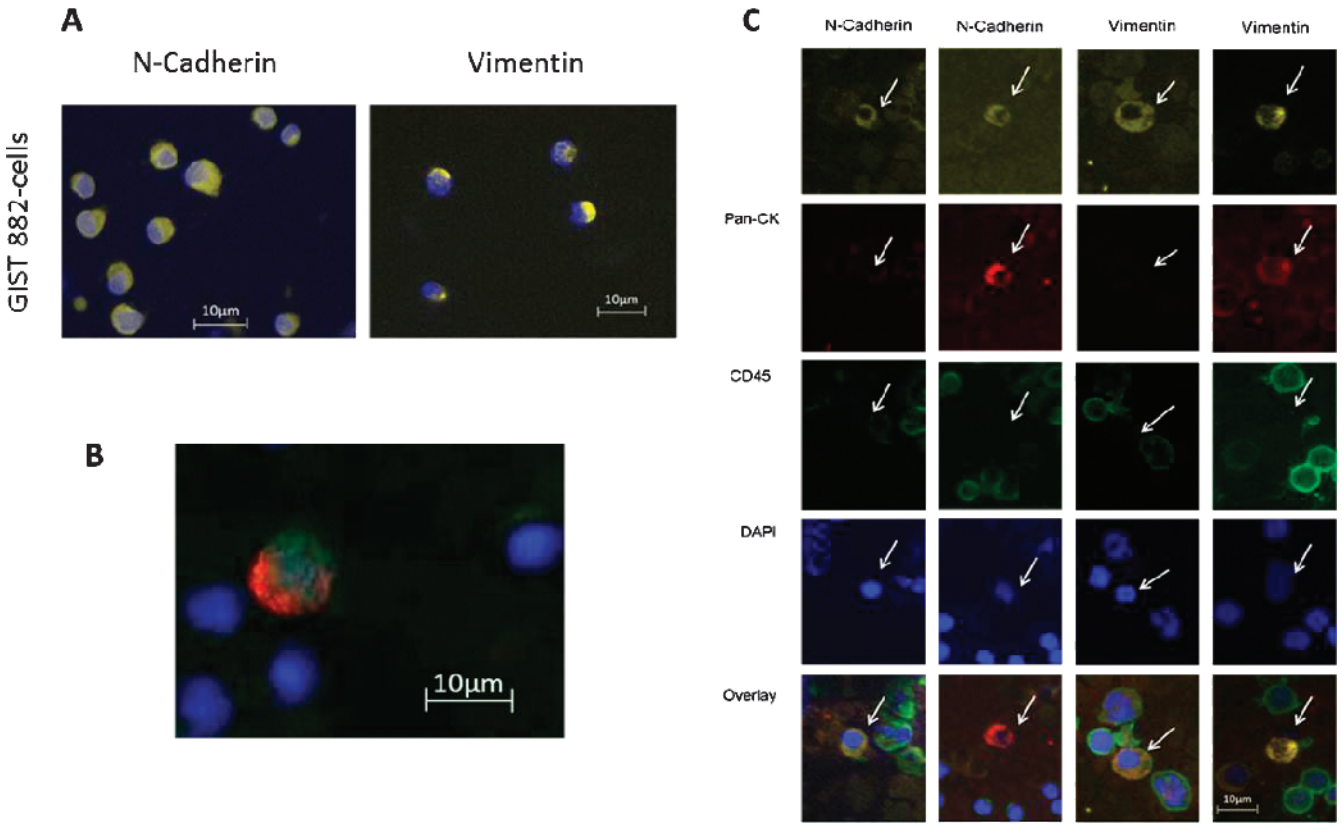

Figure 3. (A) Immunofluorescence staining of GIST 882 cells as positive control for N-cadherin (yellow) and vimentin (yellow), respectively. (B) Overlay picture of a CTC from an HCC patient showing both epithelial and mesenchymal features. This cell stained positive for pan-CK (red), N-cadherin (green), and DAPI (blue). (C) CTC subtypes showing mesenchymal and/or epithelial features.

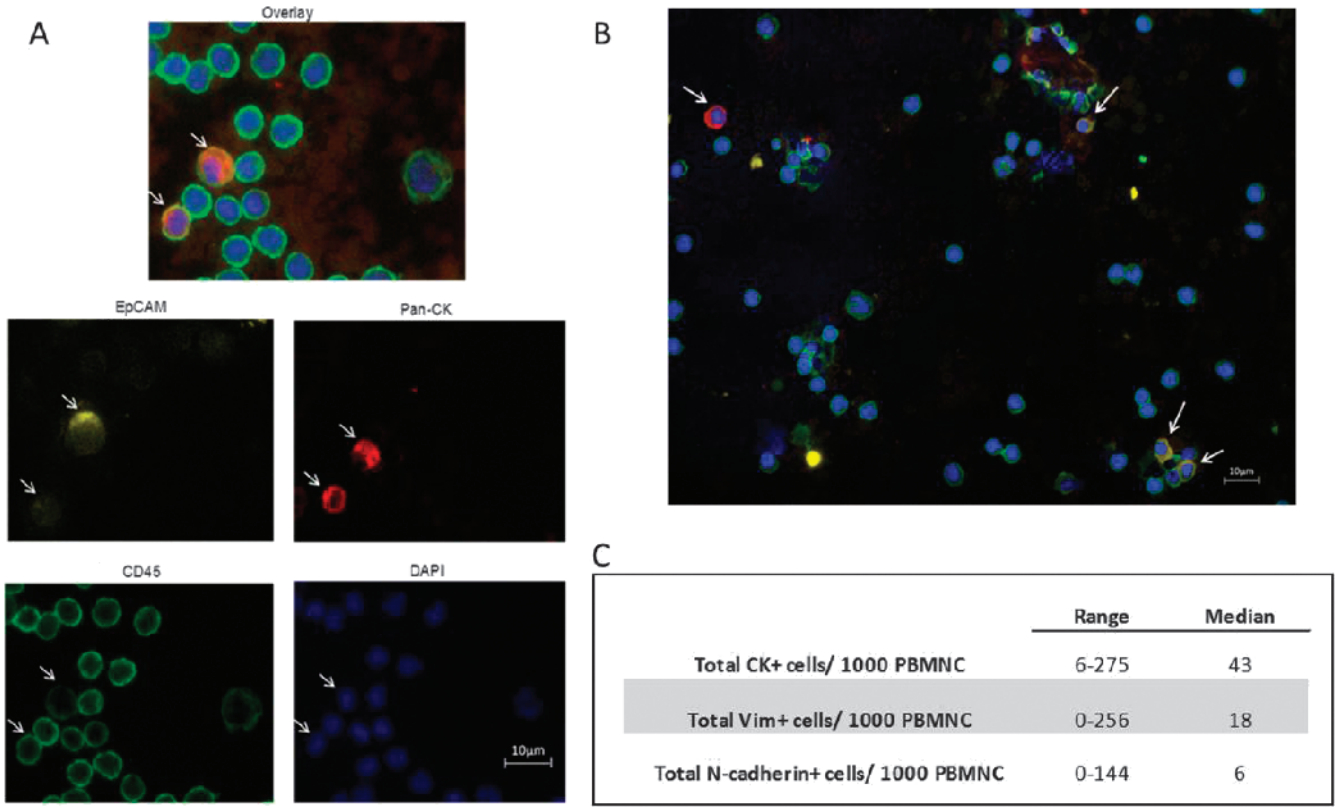

	Range	Median
Total CK+ cells/ 1000 PBMNC	6-275	43
Total Vim+ cells/ 1000 PBMNC	0-256	18
Total N-cadherin+ cells/ 1000 PBMNC	0-144	6

Figure 4. (A) Cells considered to be CTCs are indicated with a white arrow. This figure depicts the heterogeneity of detected CTC in one single HCC blood sample. Among hematopoietic CD45-positve cells, it shows two CTCs that were both pan-CK–positive (red) and CD45-positive (green), while one of them was also EpCAM-positive (yellow). All cells showed a positive nuclear staining (DAPI, blue). (B) Example of individual morphologic profile showing one epithelial (CK-positive) and three mesenchymal (N-cadherin–positive) cells. (C) CTC subtypes were summarized, normalized against the total amount of cells in the DAPI channel per visual field, and expressed in potential CTC per 1000 PBMNCs after enrichment.

was significantly correlated to cirrhosis ($P = .03$; Figure 5*B*). The amount of epithelial CK+ cells ($P = .1$) and the ratio of N-cadherin+/CK+ cells ($P = .1$) showed a by trend significant correlation to the Child status (Figure 5*C*).

To test whether the N-cadherin+/CK+ ratio or the vimentin+/CK+ ratio potentially divided patients according to their chance of a prolonged TTP, we used the Kaplan-Meier log-rank test, resulting in a significant association of both ratios with TTP. A vimentin+/CK+ ratio higher than 0.5, meaning that there were half as many vimentin-positive cells as CK+ cells, was associated with a longer median TTP [1 *vs* 15 months; $P = .03$; hazard ratio (HR) = 0.18; 95% confidence interval = 0.01–2.75]. A N-cadherin+/CK+ ratio lower than 0.1 resembled an association to shortened TTP (1 *vs* 15 months; $P = .03$; HR = 0.19; 95% confidence interval = 0.01–2.75; Figure 5*D*).

Discussion

In this study, we used multi-immunofluorescence staining to detect a significant variety in interindividual as well as intraindividual CTC characteristics. We measured epithelial cells, staining positive for pan-CK (+DAPI) but negative for EpCAM, and CD45 as well as cells staining positive for both CK and EpCAM while negative for CD45. We also detected CTC with mesenchymal properties such as vimentin and N-cadherin as well as cells with both epithelial and mesenchymal features, remarkably with changing ratios even during local ablative treatment of patients. It has very recently been described by Yu and colleagues that CTC undergo EMT during treatment and that these changes, and not only the absolute numbers of certain subgroups, correlate well with response and resistance to cytotoxic treatment, respectively [25]. The detection of CTC showing mesenchymal phenotype was also reported by Gradilone and colleagues who characterized CTC for CK and markers of EMT and found the gain of mesenchymal markers in CTC to be correlated to patient prognosis in a follow-up of 24 months [26,27]. Their data showed that the presence of mesenchymal markers on CTC more accurately predicted a poor prognosis than the expression of CK alone. Here, we were able to confirm that the presence of mesenchymal cells correlates to survival in HCC patients. However, our results in this study group indicated that an increase in epithelial cells was associated with worse treatment outcome in patients with HCC, which leads us to hypothesize that epithelial cells may be the driver of aggressiveness in this study population. Supporting these findings, we also revealed that the total amount of CK+ cells was higher in patients with cirrhosis and in patients with a worse Child status. These contradicting results may be explainable by the different entities (breast *vs* hepatocellular cancer), different treatment approaches, or a limited sample size. The shift from mesenchymal to epithelial cell profiles was significantly correlated with shortened TTP in both N-cadherin and vimentin to CK ratios, respectively, and indicated that our data might be valid despite the low patient number.

Remarkably, in our study, epithelial and mesenchymal cells were detectable in the peripheral blood of almost all patients—in different proportions—whereas only some of these patients (4/11; 36%) presented cells with both features on the same cell potentially indicating different stages of EMT. However, this patient group is too small to answer this question conclusively at this point. Additionally, a distinct proportion of cells stained positive for pan-CK and CD45 as well as for EpCAM, pan-CK, and CD45, a phenomenon already described by Yu and colleagues [24]. The additional CD45+ staining may not be exclusive for hematopoietic cells but may hypothetically be acquired during dormant stay in the bone marrow or through effects comparable to trogocytosis, i.e., transfer of membrane proteins [28]. Therefore, depletion of CD45-positive cells might lead to a loss of cells of interest during the negative enrichment procedure. Moreover, the retrieval was significantly lower after immunomagnetic depletion compared to density gradient centrifugation alone as shown by our spiking experiments. Though when anticipating CTC isolation from blood recapturing spiked cultured cells it remains unclear to which extent these experiments reflect the *in vivo* situation. CD45 depletion will be omitted in the following studies to obtain an increased CTC recovery rate. After determining the total amount of cells, samples will be spun onto the required amount of slides with maximum of 5×10^6 cells per slide that will lead to a higher number of slides with increased staining options allowing to investigate a wider range of cell type characteristics. Even though the depletion rate was not very effective, we chose to proceed with the protocol to diminish hematopoietic cells and to be able to overlook different cell types within blood samples. Moreover, our method is based on cell type ratios rather than absolute cell numbers assuming that a loss of potential CTC might not affect the proportion of their CD45-negative subtypes. These questions need to be addressed in subsequent investigations analyzing a higher number of blood samples and multiple CTC subtypes also including endothelial, stem cell, and other characteristics.

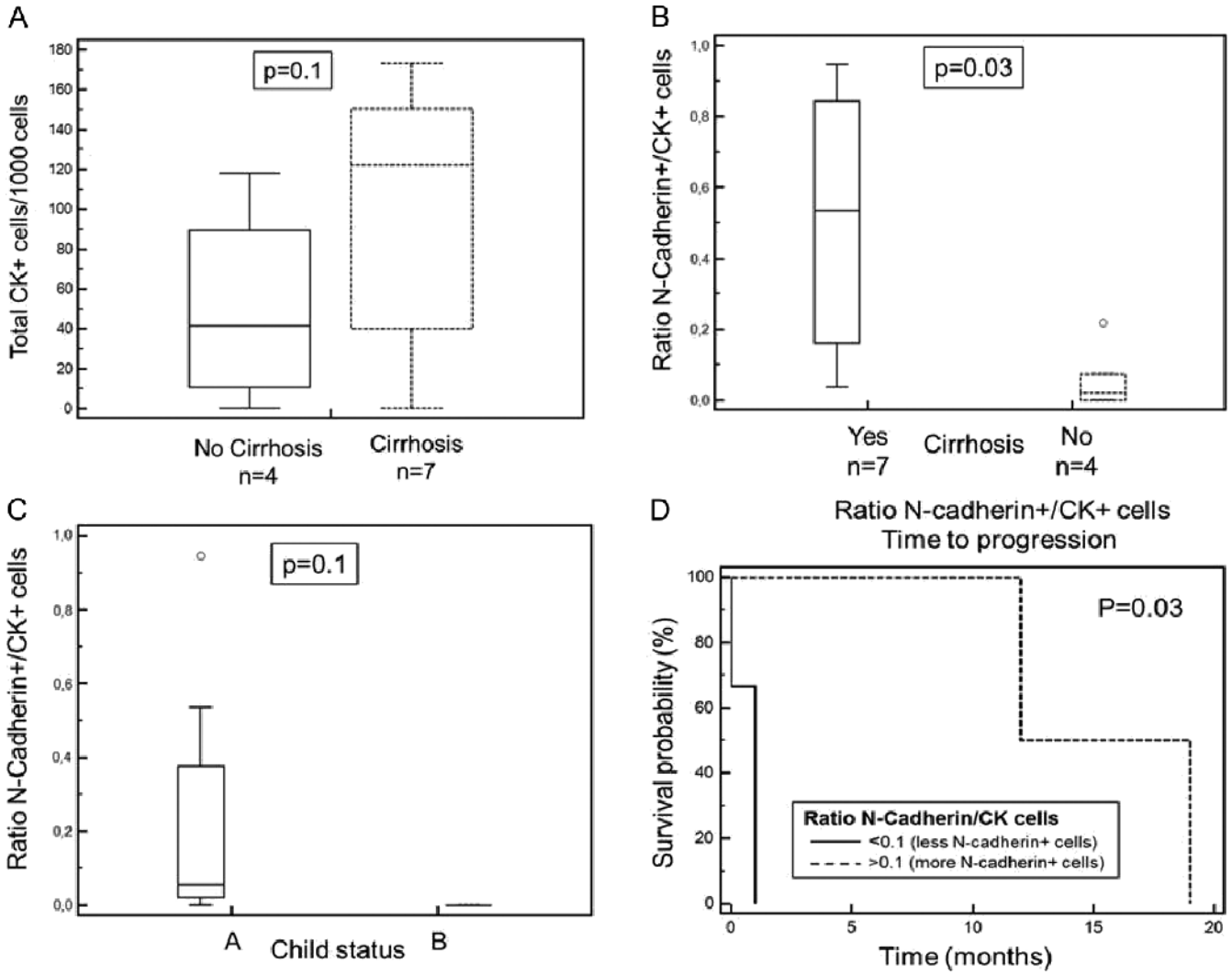

Figure 5. (A) The total amount of CK+ cells/1000 PBMNCs was higher in patients with cirrhosis compared to patients without cirrhosis ($P = .1$). (B) The ratio of N-cadherin+/CK+ cells was also correlated to cirrhosis. Patients with cirrhosis had a higher total amount of CK+ cells that led to a lower ratio of N-cadherin+/CK+ cells compared to patients without cirrhosis ($P = .03$). (C) The ratio of N-cadherin+/CK+ cells was correlated to the Child status ($P = .1$). (D) Association of high *vs* low N-cadherin+/CK+ CTC ratio with TTP employing Kaplan-Meier log-rank test ($P = .03$; HR = 0.18).

In contrast to CTC in other entities being commonly described to have a large cellular size and a high nuclear to cytoplasmic ratio [14], our results confirm a previous report from a patient with breast cancer by Marrinucci and colleagues showing a wide range of signal intensities and a variety of cell sizes [29,30]. This is of relevance because the isolation by size of epithelial tumor cells using the ISET System (Rarecells, Paris, France) is one of the few major (semi) automated approaches used for detecting CTC. Vona et al. used ISET in patients with HCC to evaluate its clinical impact. Fifty-two percent of a total of 44 patients had detectable CTC and their prevalence was significantly correlated with the presence of multifocal tumors, portal tumor thrombosis, and Child-Pugh class B/C [15]. In a study of Schulze and colleagues, the CellSearch System was applied to detect EpCAM-positive CTC in the blood of HCC patients resulting in a detection rate of 45% (14 of 31 HCC patients) and a significant correlation between the detection of epithelial CTC and pathologic AFP values [17]. Xu et al. reported the development and validation of an EpCAM-independent magnetic cell separation system mediated by the interaction of the ASGPR1 exclusively expressed on hepatocytes with its ligand. CTCs were then identified by Hep-Par-1 staining. An average of 24 ± 19 CTCs per 5 ml of blood was detected in 81% of HCC patients, suggesting that the variation ranged from one to nine tumor cells per milliliter in the examined patients. Therefore, with this study, we wanted to show that the individual cell composition and especially changes in this personal cell profile implicate alternating therapeutic responses, potentially with more sensitivity than currently available. Furthermore, these changes may lead to specific treatments, aiming at distinct CTC profiles.

Taken together, our data support the hypothesis that different CTC populations are identifiable in the peripheral blood of patients with HCC and that these individual cell type profiles may have distinct clinical implications. This method offers an opportunity to detect changes in the composition of circulating non-hematopoietic cells in the blood of patients with HCC and, therefore, to create an individual profile of each patient, which might help to predict patient outcome and potentially to select the appropriate treatment. Further studies including systemic treatments of HCC seem to be warranted.

Acknowledgments

We thank Sabine Kasimir-Bauer and her team (Department of Gynecology and Obstetrics, University Hospital Essen) for supporting the validation of our method using the ARIOL-SL System. We also thank Karl Lang (Institute of Immunology, University Hospital Essen) for constantly granting us access to his Keyence all-in-one fluorescence microscope. Furthermore, we thank Sebastian Bauer and his team (Department of Medical Oncology, University Hospital Essen) for the supply of GIST 882 cells.

References

[1] Llovet JM, Burroughs A, and Bruix J (2003). Hepatocellular carcinoma. *Lancet* **362**, 1907–1917.

[2] Jemal A, Bray F, Center MM, Ferlay J, Ward E, and Forman D (2011). Global cancer statistics. *CA Cancer J Clin* **61**, 69–90.

[3] Belghiti J, Panis Y, Farges O, Benhamou JP, and Fekete F (1991). Intrahepatic recurrence after resection of hepatocellular carcinoma complicating cirrhosis. *Ann Surg* **214**, 114–117.

[4] Arriagada R, Bergman B, Dunant A, Le Chevalier T, Pignon JP, and Vansteenkiste J (2004). Cisplatin-based adjuvant chemotherapy in patients with completely resected non–small-cell lung cancer. *N Engl J Med* **350**, 351–360.

[5] Winton T, Livingston R, Johnson D, Rigas J, Johnston M, Butts C, Cormier Y, Goss G, Inculet R, Vallieres E, et al. (2005). Vinorelbine plus cisplatin vs. observation in resected non–small-cell lung cancer. *N Engl J Med* **352**, 2589–2597.

[6] Olaussen KA, Dunant A, Fouret P, Brambilla E, André F, Haddad V, Taranchon E, Filipits M, Pirker R, Popper HH, et al. (2006). DNA repair by ERCC1 in non–small-cell lung cancer and cisplatin-based adjuvant chemotherapy. *N Engl J Med* **355**, 983–991.

[7] Sangro B, Bilbao JI, Boan J, Martinez-Cuesta A, Benito A, Rodriguez J, Panizo A, Gil B, Inarrairaegui M, Herrero I, et al. (2006). Radioembolization using 90Y-resin microspheres for patients with advanced hepatocellular carcinoma. *Int J Radiat Oncol Biol Phys* **66**, 792–800.

[8] Lau WY, Lai EC, and Leung TW (2011). Current role of selective internal irradiation with yttrium-90 microspheres in the management of hepatocellular carcinoma: a systematic review. *Int J Radiat Oncol Biol Phys* **81**, 460–467.

[9] Sun YF, Yang XR, Zhou J, Qiu SJ, Fan J, and Xu Y (2011). Circulating tumor cells: advances in detection methods, biological issues, and clinical relevance. *J Cancer Res Clin Oncol* **137**, 1151–1173.

[10] Lianidou ES and Markou A (2011). Circulating tumor cells in breast cancer: detection systems, molecular characterization, and future challenges. *Clin Chem* **57**, 1242–1255.

[11] Hou JM, Krebs M, Ward T, Sloane R, Priest L, Hughes A, Clack G, Ranson M, Blackhall F, and Dive C (2011). Circulating tumor cells as a window on metastasis biology in lung cancer. *Am J Pathol* **178**, 989–996.

[12] Zhang N, Li X, Wu CW, Dong Y, Cai M, Mok MT, Wang H, Chen J, Ng SS, Chen M, et al. (2012). microRNA-7 is a novel inhibitor of YY1 contributing to colorectal tumorigenesis. *Oncogene*. DOI: 10.1038/onc.2012.526, E-pub ahead of print.

[13] Waguri N, Suda T, Nomoto M, Kawai H, Mita Y, Kuroiwa T, Igarashi M, Kobayashi M, Fukuhara Y, and Aoyagi Y (2003). Sensitive and specific detection of circulating cancer cells in patients with hepatocellular carcinoma; detection of human telomerase reverse transcriptase messenger RNA after immunomagnetic separation. *Clin Cancer Res* **9**, 3004–3011.

[14] Xu W, Cao L, Chen L, Li J, Zhang XF, Qian HH, Kang XY, Zhang Y, Liao J, Shi LH, et al. (2011). Isolation of circulating tumor cells in patients with hepatocellular carcinoma using a novel cell separation strategy. *Clin Cancer Res* **17**, 3783–3793.

[15] Vona G, Estepa L, Beroud C, Damotte D, Capron F, Nalpas B, Mineur A, Franco D, Lacour B, Pol S, et al. (2004). Impact of cytomorphological detection of circulating tumor cells in patients with liver cancer. *Hepatology* **39**, 792–797.

[16] Guo J, Yao F, Lou Y, Xu C, Xiao B, Zhou W, Chen J, Hu Y, and Liu Z (2007). Detecting carcinoma cells in peripheral blood of patients with hepatocellular carcinoma by immunomagnetic beads and RT-PCR. *J Clin Gastroenterol* **41**, 783–788.

[17] Schulze K, Beneken C, Staufer K, Nashan B, Lohse AW, Pantel K, Riethdorf S, and Wege H (2011). Detection of Epcam-positive circulating tumor cells in patients with hepatocellular carcinoma—a pilot study. *Hepatology* **54**, 1357a.

[18] Krebs MG, Hou JM, Sloane R, Lancashire L, Priest L, Nonaka D, Ward TH, Backen A, Clack G, Hughes A, et al. (2012). Analysis of circulating tumor cells in patients with non-small cell lung cancer using epithelial marker-dependent and -independent approaches. *J Thorac Oncol* **7**, 306–315.

[19] Ignatiadis M, Georgoulias V, and Mavroudis D (2008). Circulating tumor cells in breast cancer. *Curr Opin Obst Gynecol* **20**, 55–60.

[20] Ignatiadis M, Georgoulias V, and Mavroudis D (2008). Micrometastatic disease in breast cancer: clinical implications. *Eur J Cancer* **44**, 2726–2736.

[21] Hoffmann A-C (2009). A three-gene signature for outcome in soft tissue sarcoma. *Clin Cancer Res* **15**, 6472.

[22] Hoffmann A-C, Mori R, Vallbohmer D, Brabender J, Klein E, Drebber U, Baldus SE, Cooc J, Azuma M, Metzger R, et al. (2008). High expression of HIF1a is a predictor of clinical outcome in patients with pancreatic ductal adenocarcinomas and correlated to PDGFA, VEGF, and bFGF. *Neoplasia* **10**, 674–679.

[23] Hoffmann A-C, Wild P, Leicht C, Bertz S, Danenberg KD, Danenberg PV, Stoehr R, Stoeckle M, Lehmann J, Schuler M, et al. (2010). MDR1 and ERCC1 expression predict outcome of patients with locally advanced bladder cancer receiving adjuvant chemotherapy. *Neoplasia* **12**, 628–636.

[24] Yu M, Stott S, Toner M, Maheswaran S, and Haber DA (2011). Circulating tumor cells: approaches to isolation and characterization. *J Cell Biol* **192**, 373–382.

[25] Yu M, Bardia A, Wittner BS, Stott SL, Smas ME, Ting DT, Isakoff SJ, Ciciliano JC, Wells MN, Shah AM, et al. (2013). Circulating breast tumor cells

exhibit dynamic changes in epithelial and mesenchymal composition. *Science* **339**, 580–584.

[26] Gradilone A, Raimondi C, Nicolazzo C, Petracca A, Gandini O, Vincenzi B, Naso G, Agliano AM, Cortesi E, and Gazzaniga P (2011). Circulating tumour cells lacking cytokeratin in breast cancer: the importance of being mesenchymal. *J Cell Mol Med* **15**, 1066–1070.

[27] Raimondi C, Gradilone A, Naso G, Vincenzi B, Petracca A, Nicolazzo C, Palazzo A, Saltarelli R, Spremberg F, Cortesi E, et al. (2011). Epithelial-mesenchymal transition and stemness features in circulating tumor cells from breast cancer patients. *Breast Cancer Res Treat* **130**, 449–455.

[28] Joly E and Hudrisier D (2003). What is trogocytosis and what is its purpose? *Nat Immunol* **4**, 815.

[29] Allard WJ, Matera J, Miller MC, Repollet M, Connelly MC, Rao C, Tibbe AG, Uhr JW, and Terstappen LW (2004). Tumor cells circulate in the peripheral blood of all major carcinomas but not in healthy subjects or patients with nonmalignant diseases. *Clin Cancer Res* **10**, 6897–6904.

[30] Marrinucci D, Bethel K, Bruce RH, Curry DN, Hsieh B, Humphrey M, Krivacic RT, Kroener J, Kroener L, Ladanyi A, et al. (2007). Case study of the morphologic variation of circulating tumor cells. *Hum Pathol* **38**, 514–519.